Available online at www.sciencedirect.com
ScienceDirect
Polymer 47 (2006) 7711–7719
polymer
www.elsevier.com/locate/polymer

Multiwalled carbon nanotube/polybenzoxazine nanocomposites: Preparation, characterization and properties

Qiao Chen [c], Riwei Xu [a,b], Dingsheng Yu [a,b,*]

[a] *The Key Laboratory of Beijing City on Preparation and Processing of Novel Polymer Materials, Beijing University of Chemical Technology, Beijing 100029, PR China*
[b] *Key Laboratory for Nanomaterials, Ministry of Education, Beijing University of Chemical Technology, Beijing 100029, PR China*
[c] *College of Chemical Engineering and Materials, Zhejiang University of Technology, Hangzhou 310014, PR China*

Received 7 December 2005; received in revised form 22 August 2006; accepted 23 August 2006
Available online 18 September 2006

Abstract

A novel nanocomposite composed of polybenzoxazine (PBZ) and multiwalled carbon nanotubes (MWNT) was prepared successfully. The surface modification of MWNT, including nitric acid modification followed by toluene-2,4-diisocyanate (TDI) treatment, introduced hydroxyl, carboxyl, and isocyanate groups on the MWNT surface. The surface carboxyl groups catalyzed the ring-opening reaction of benzoxazine and thus decreased the curing temperature of the system. The isocyanate groups reacted with the phenolic hydroxyl groups generated by the ring opening of benzoxazine resulting in the significant improvement of the adhesion between PBZ and MWNT. Dynamic mechanical analyses indicated the increase of storage modulus as well as T_g by the addition of MWNT into PBZ. A well dispersed modified-MWNT on nanoscale level inside PBZ matrix was observed by TEM and SEM.

Keywords: Polybenzoxazine; Multiwalled carbon nanotubes; Nanocomposite

1. Introduction

Carbon nanotubes (CNTs) are hexagonal array of rolled carbon sheets with several microns in length and a few nanometers in diameter. Based on the number of carbon layers through the wall, either singlewalled carbon nanotubes (SWNT) or multiwalled carbon nanotubes (MWNT) could form [1,2]. CNTs exhibit remarkable stiffness, strength and conductivity because of the graphitic nature of the nanotube lattice. Both theoretical and experimental results suggest that the elastic modulus of carbon nanotubes may exceed 1.0 TPa [3,4] and the tensile strength is in the range of 10–50 GPa [5,6]. Owing to its remarkable properties, CNTs have attracted extensive attention for its potential applications in various fields, especially as the reinforcement in composites consisted of polymers [7–12]. The studies on CNTs-reinforced polymer materials have been reported for various kinds of organic polymers [13–40].

The key issue in the effective utilization of CNTs in nanocomposites is to control deaggregation and dispersion of CNTs throughout the polymer matrices, which correlated with mechanical properties [41] and conductivity [42]. It has been reported that the strength, stiffness, and conductivity could be greatly improved by the addition of CNTs with relatively low concentration [43–46]. However, in most of the cases, homogeneous dispersion of CNTs is hindered by the ''entangled'' and ''aggregated'' structures of CNTs, due to the Van der Waals interactions among tubes combined with their high surface area and aspect ratio. Furthermore, the nonactive surface of the CNTs also limits its application due to the lack of adhesion between CNTs and polymer matrices. It has been suggested that the chemical modification of CNTs surface, such as

* Corresponding author. The Key Laboratory of Beijing City on Preparation and Processing of Novel Polymer Materials, Beijing University of Chemical Technology, Beijing 100029, PR China. Tel.: +86 10 64434849; fax: +86 10 64433718.
E-mail address: yuds@mail.buct.edu.cn (D. Yu).

0032-3861/$ - see front matter © 2006 Elsevier Ltd. All rights reserved.
doi:10.1016/j.polymer.2006.08.058

through acid treatment and the incorporation of functional groups, improved the homogeneous dispersion of CNTs in the matrices [13–17,44].

Polybenzoxazine, as a new kind of thermosetting phenolic resin, has been known for its unique characteristics, such as self-fire-extinguishing property, low moisture absorption, better static and dynamic mechanic property as well as excellent dimensional stability. Benzoxazine monomers as the polybenzoxazine precursors can be easily prepared from inexpensive raw materials like phenols, formaldehyde, and primary amines. Accordingly, they have a tremendous flexibility in molecular design for monomers and consequently a versatile performance for polymers. Furthermore, polybenzoxazines can be obtained by polymerizing the corresponding benzoxazine monomers at elevated temperatures through heterocyclic ring opening, without using strong acid or basic catalysts and releasing byproducts [47–55].

The improvement in the properties of polybenzoxazine has been expected and required; so various studies have been carried out. It has been shown that the mechanical property of polybenzoxazine can be reinforced by the addition of glass-fiber [56] or carbon fiber [57,58]. Introduction of organically modified montmorillonite (OMMT) significantly decreased the curing temperature of benzoxazine monomer while increased storage modulus, T_g, and thermal stability of the matrix [59–64]. Lee et al. [65,66] reported the synthesis and properties of benzoxazine-containing polyhedral oligomeric silsesquioxane (POSS) monomer, which can copolymerize with other benzoxazine monomers through ring-opening polymerization. Thermal properties of these POSS-containing polybenzoxazine nanocomposites have been improved over the pure resin.

However, an examination of literatures indicated that no study has been done on CNTs/polybenzoxazine nanocomposite. In the present studies, a novel MWNT/polybenzoxazine nanocomposite was prepared via a solvent method for the first time. The nitric acid modification followed by toluene-2,4-diisocyanate (TDI) treatment of MWNT and an ultra-sonic vibration were used to achieve homogeneous dispersion of MWNT throughout polybenzoxazine matrix. The effects of the MWNT concentration on curing temperature of the benzoxazine monomer as well as dynamic mechanical properties of the matrix were investigated; the curing behavior of benzoxazine monomer in the presence of MWNT was also discussed.

2. Experimental

2.1. Materials

Bisphenol A was purchased from Haidian Xingxing Reagent Plant Beijing; paraformaldehyde and aniline from Chemical Reagent Institute Tianjin; nitric acid (65%), tetrahydrofuran (THF) and acetone from Beijing Chemical Reagent Co. Ltd. Toluene-2,4-diisocyanate (TDI) was obtained from Shanghai Chemical Reagent Plant. Stannous octoate was purchased from Beijing Hanfeng Polyurethane Co. MWNT (95%), which was chemical vapor deposition materials with a diameter of 10–30 nm and length 5–15 μm, was supplied by Shenzhen Nanotech Port Co. Ltd, and the transmission electron microscope photo of the MWNT is shown in Fig. 1. All reagents were used as received without further purification.

2.2. Preparation of samples

The modified-MWNT was obtained by first treating with nitric acid followed by excess TDI. The acid treatment of MWNT was carried out by mixing 5 g MWNT with 200 ml concentrated nitric acid (65%). The mixture was stirred for 1 h at 120 °C, and then the MWNT was filtered and washed with distilled water until the pH of the filtrate reaches 7. The solid product was dried under vacuum (25 mmHg) at 50 °C for 24 h. Dried acid-treated MWNT (0.5 g) was added to the mixture containing 10 g TDI and 0.1 ml stannous octoate. The resulting mixture was then stirred under N_2 for 4 h at 80 °C. The final product was filtered, washed three times with acetone, and dried under 25 mmHg vacuum at 50 °C for 24 h.

Bis(3-phenyl-3,4-dihydro-2H-1,3-benzoxazine)isopropane monomer (BZ) was prepared from aniline, paraformaldehyde, and bisphenol A by using solvent method as described in previous paper [47]. The structure of the BZ and polybenzoxazine therefore, abbreviated as PBZ, is shown in Scheme 1.

The PBZ/MWNT nanocomposites were prepared via a solvent method. Certain amount of modified-MWNT was added into the system composed of 5.0 g BZ monomer and 10 ml THF. The weight ratios of BZ to MWNT were between 99.8/0.2 and 98/2. In order to achieve homogeneous dispersion of the modified-MWNT into PBZ, the resulting mixtures of MWNT and BZ were stirred for 10 h at room temperature and sonicated for 2 h at 40 °C. After treating the mixtures at 80 °C for 5 h to evaporate the portion of THF, they were put into the steel molds and melt at 100 °C. The molds were heated with the following step cure cycles: 160 °C for 1 h, 180 °C for 2 h, 200 °C for 1 h, and 220 °C for 1 h in an air-circulating oven. The size of the molded samples was 25 × 5 × 1 mm.

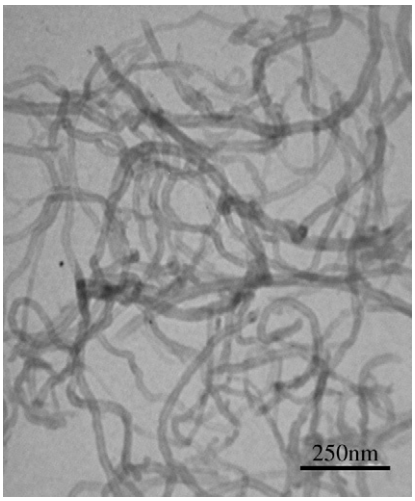

Fig. 1. TEM image of the as-received MWNT.

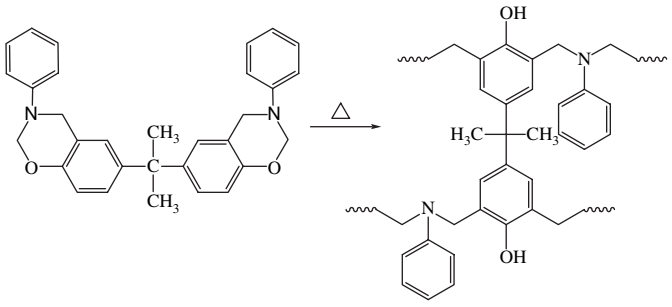

Scheme 1. Preparation of polybenzoxazine from typical benzoxazine monomer.

2.3. Sample analysis

A Thermo Electron Corporation-ESCALAB 250 X-ray photoelectron spectrometer (XPS) equipped with Al Kα 200 W was used to analyze elemental compositions of MWNT surface. A Nicolet-60SXB infrared spectrometer (IR) was used to characterize the surface of modified-MWNT and monitor the curing behavior of the BZ monomer in the presence of MWNT. All the samples were analyzed in the form of KBr disc. The functional groups attached to the modified-MWNT were verified by a Bruker Avance 600 MHZ nuclear magnetic resonance (NMR) spectrometer in $CDCl_3$. The curing temperature of BZ monomer was measured by a Perkin–Elmer differential scanning calorimetry (DSC) at a heating rate of 10 °C/min under nitrogen. The distribution of the MWNT inside the PBZ was examined by a Hitachi H-800-1 transmission electron microscope (TEM) using an acceleration voltage of 200 kV and a FEI XL-30 field emission scanning electron microscope (SEM). The TEM sample was prepared by ultramicrotome and placed in 200 mesh copper grids for analysis. SEM was performed on fractured surfaces of block samples. Dynamic mechanical analyses (DMA) were conducted on Rheometric Scientific™ DMTA V at 1 Hz at a heating rate of 3 °C/min. The DMA samples were the molded ones.

3. Results and discussions

3.1. Characterization of modified-MWNT

The elemental compositions of modified-MWNT were characterized by XPS. Fig. 2 shows C_{1s}, O_{1s}, and N_{1s} XPS spectra of the MWNT treated by nitric acid and TDI. The C_{1s} spectrum of pure MWNT exhibited a peak at 284.3 eV, which was assigned to an sp^2 carbon. The O_{1s} spectrum showed a peak at 533.7 eV, which was corresponding to the ether-type group with oxygen singly bonded to carbon [37,38]. Comparing Fig. 2(A) and (B), the acid treatment not only resulted in the broadening and asymmetry of C_{1s} peak, but also increased the intensity of O_{1s} peak. Thus, both the carbon and oxygen atoms on the MWNT surface had higher binding energies. The TDI modification hardly affected O_{1s} peak while made C_{1s} peak broadening further because of the more diverse environment of the carbon atoms, and increased the intensity of N_{1s} peak significantly, as shown in Fig. 2(C).

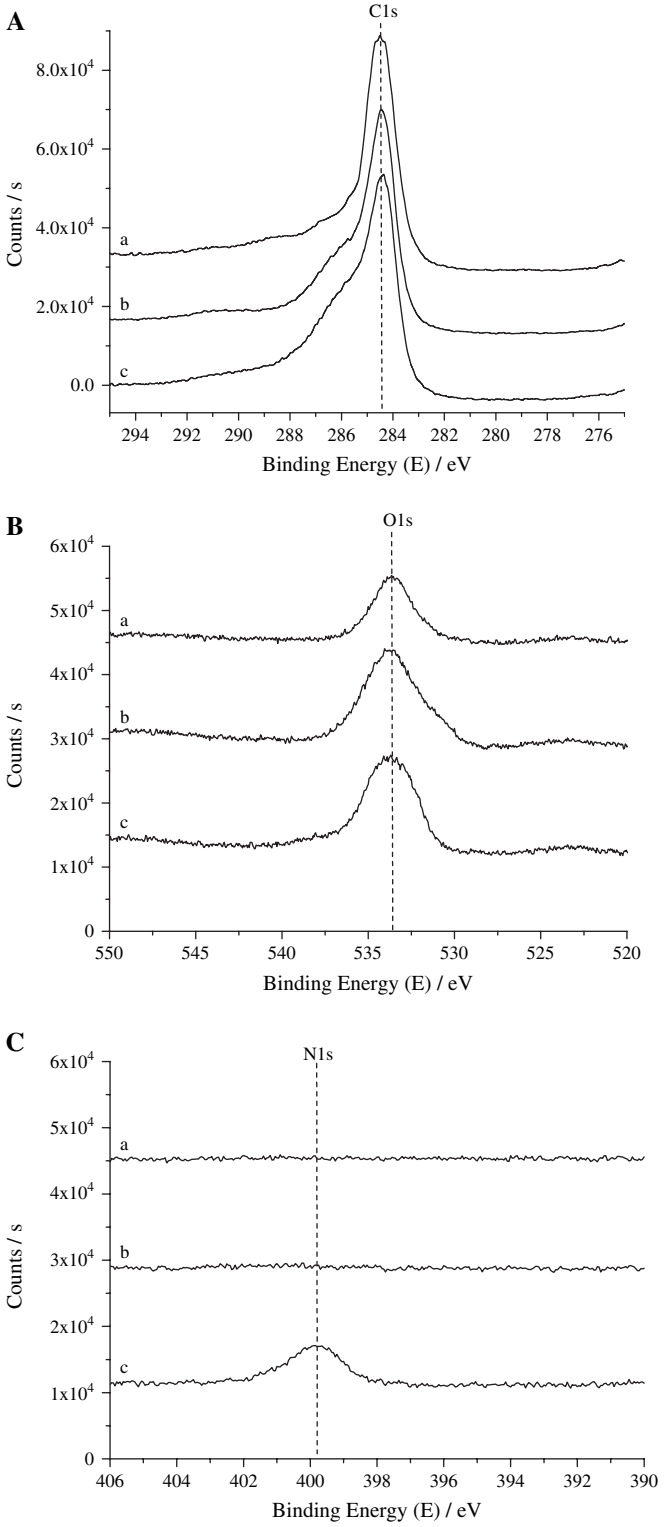

Fig. 2. XPS (A) C_{1s}, (B) O_{1s} and (C) N_{1s} core-level scan spectra of MWNT, (a) pure MWNT, (b) treated with nitric acid and (c) modified by TDI.

The chemical compositions of the modified-MWNT as well as atomic molar ratios of O/C and N/C for each sample are summarized in Table 1. Nitric acid treatment caused the decrease of the carbon relative concentration while increased oxygen relative concentration, which suggested the presence of oxygen containing groups. TDI modification resulted in

Table 1
Chemical composition of the MWNT

Sample	Atomic relative concentration (%)			Atomic molar ratio (%)	
	C	O	N	O/C	N/C
Pure MWNT	92.86	7.14	0	5.77	0
Treated by nitric acid	85.1	13.43	1.46	11.84	1.47
Modified by TDI	81.72	13.53	4.75	12.42	4.98

the increasing nitrogen relative atomic concentration, which indicated the introduction of nitrogen containing structures on the MWNT surface.

The infrared spectra of the modified-MWNT are shown in Fig. 3. The bands at 1705 and 1173 cm^{-1} were due to the

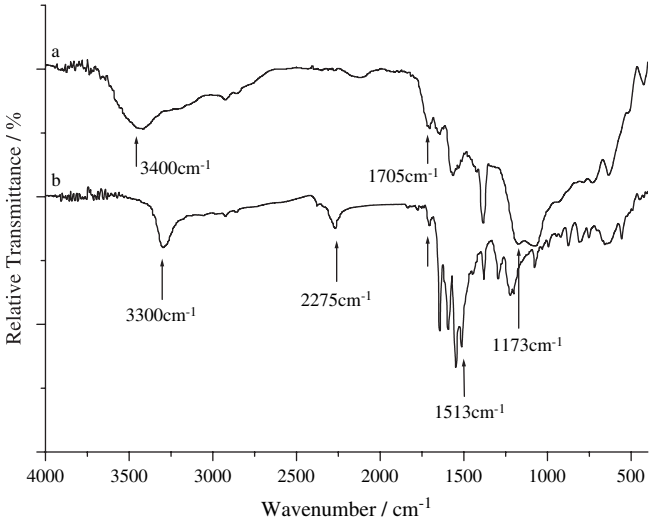

Fig. 3. IR of modified-MWNT treated with (a) nitric acid and (b) TDI.

−C═O and −C−O− stretching, respectively; the bands at 3300 and 3400 cm^{-1} were assigned to secondary amine group and −OH stretching vibration, respectively. Amido group gave a band at 1513 cm^{-1}. The band at 2275 cm^{-1} was due to isocyanate group, −N═C═O. The presence of bands at 1705, 1173, and 3400 cm^{-1}, as shown in Fig. 3(a), indicated that the acid treatment introduced the −OH and −COOH groups on the surface of the MWNT. Fig. 3(b) shows the IR spectrum of the TDI modified-MWNT. Both the disappearance of the bands at 1173 and 3400 cm^{-1} and the appearance of the new bands at 3300 and 1513 cm^{-1} indicated that the −OH on the MWNT surface could react with TDI to form −CO−NH−. Because of the excess of TDI, some isocyanate groups could be introduced on the MWNT surface, which resulted in the appearance of a band at 2275 cm^{-1}. The proposed surface modification reactions of MWNT are shown in Scheme 2. Furthermore, the absorption at 1705 cm^{-1} due to the structure of −C═O was still observed indicating the existence of carboxyl groups on the CNTs surface.

In order to verify the proposed formulas in Scheme 2, the functional groups attached to the nitric acid and TDI-treated MWNT were determined by NMR analysis. In the ^1H NMR of the nitric acid-treated MWNT (Fig. 4(A)), the characteristic protons of −OH and −COOH were detected at 2.02 and 7.70 ppm, respectively. Fig. 4(B) shows the ^1H NMR of the TDI modified-MWNT. With the comparison of Fig. 4(A) and (B), it was found that after the further modification of TDI, the phenyl groups, −CO−NH− and $-CH_3$ were identified as peaks at 7.02−7.17 ppm as multiple, 6.38 ppm and 2.28 ppm, respectively. The hydroxyl peak was hardly detectable in the corresponding ^1H NMR spectrum, but the protons of carboxyl groups could still be detected, which were in agreement with the result of IR.

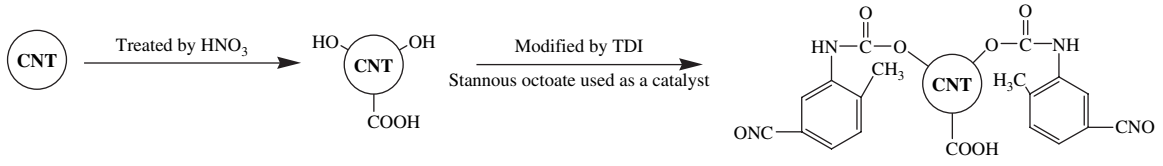

Scheme 2. The modification of MWNT.

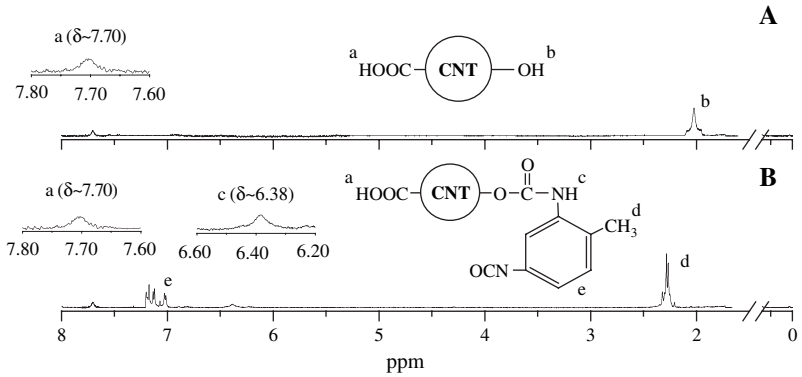

Fig. 4. ^1H NMR spectra of (A) the nitric acid-treated MWNT in $CDCl_3$ and (B) the TDI-treated MWNT in $CDCl_3$.

3.2. Curing behavior of BZ/MWNT mixture

The curing behavior of BZ monomer in the presence of modified-MWNT was monitored by DSC and IR. Fig. 5 shows the DSC curves of pure BZ monomer and BZ/MWNT mixture (ratio of 98/2) after each cure cycle. Comparing to the pure BZ monomer, with the addition of modified-MWNT, the exotherm of mixture shifted to the lower temperature range. For BZ/MWNT shown in Fig. 5(b)–(e), both the exotherm and enthalpy of the mixture gradually decreased along the curing process and finally disappeared or reached zero, which indicated that the curing reaction was completed after the 220 °C cure cycle.

Fig. 6 shows the IR spectra of BZ/MWNT mixture after different stages of curing. The initial BZ/MWNT mixture gave the −N=C=O band at 2275 cm^{-1} and BZ bands of asymmetric C−O−C stretching at 1231 cm^{-1}, CH_2 wagging at 1326 cm^{-1}, and tri-substituted benzene ring stretching at 945 and 1496 cm^{-1}. As the curing processes occurred, both

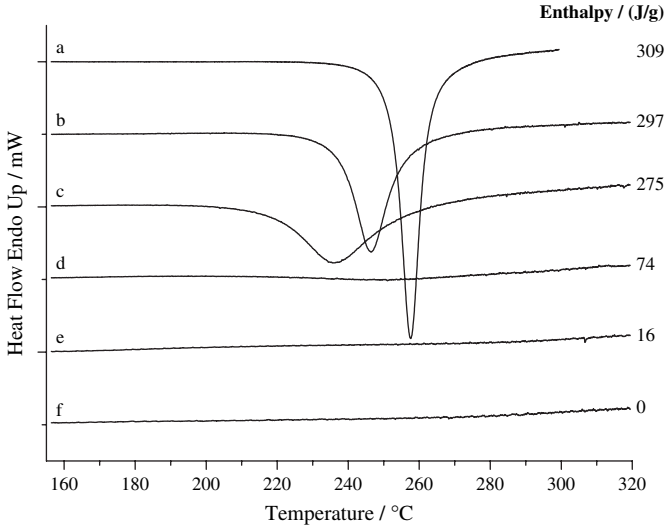

Fig. 5. DSC of (a) pure BZ monomer; (b) BZ/MWNT mixture (98/2) and the mixture after treatment at (c) 160 °C/1 h; (d) 160 °C/1 h and 180 °C/2 h; (e) 160 °C/1 h, 180 °C/2 h and 200 °C/1 h; (f) 160 °C/1 h, 180 °C/2 h, 200 °C/1 h and 220 °C/1 h.

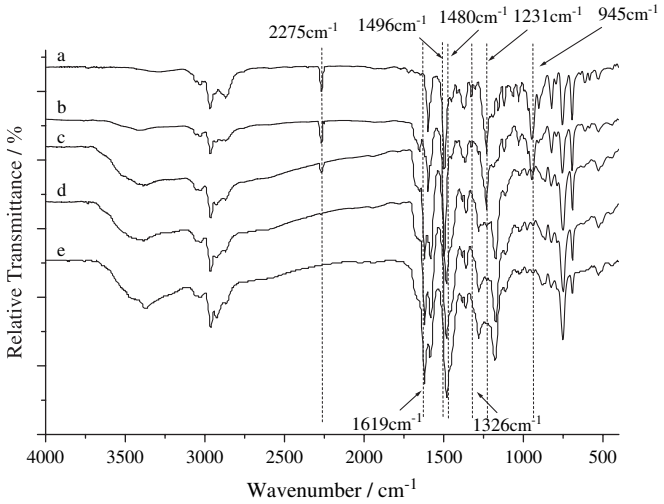

Fig. 6. IR spectra of (a) BZ/MWNT mixture (98/2) and the mixture after treatment at (b) 160 °C/1 h; (c) 160 °C/1 h and 180 °C/2 h; (d) 160 °C/1 h, 180 °C/2 h and 200 °C/1 h; (e) 160 °C/1 h, 180 °C/2 h, 200 °C/1 h and 220 °C/1 h.

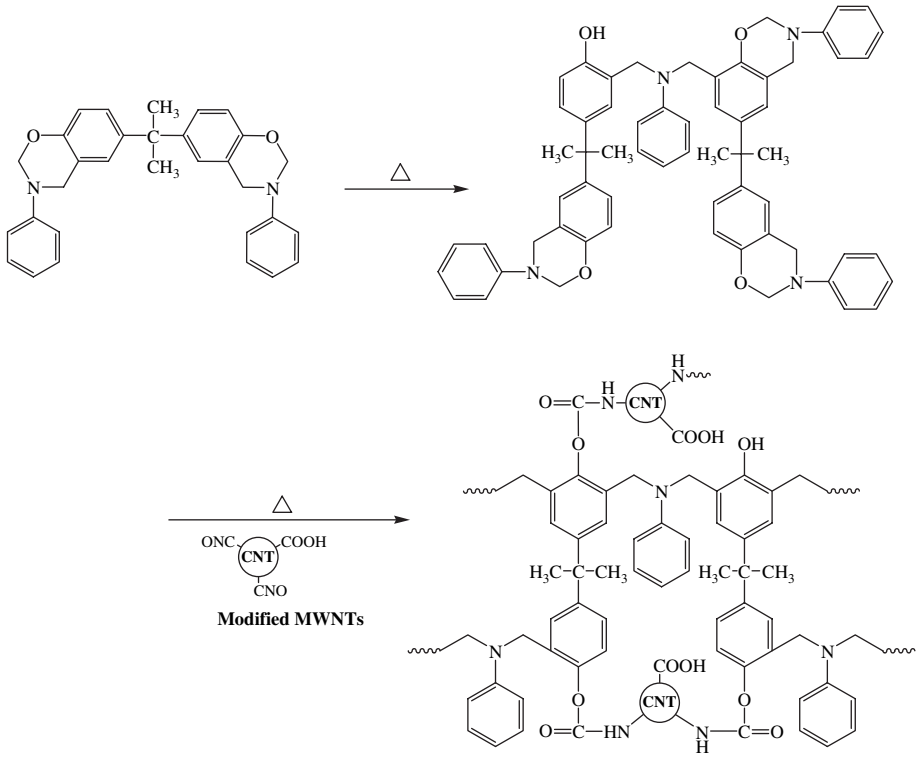

Scheme 3. Curing reaction of BZ monomer with the presence of modified-MWNT.

−N═C═O band and BZ bands decreased while two new bands at 1480 and 1619 cm^{-1} emerged. It was reported [67,68] that the peak at 1480 cm^{-1} appeared due to the tetra-substituted benzene ring mode after the curing cycle of 160 °C/1 h suggesting that the ring opening of BZ monomer afforded polybenzoxazine, which resulted in the generation of phenolic hydroxyl groups. The band at 1619 cm^{-1}, which appeared after 180 °C cure stage, was considered as amido group, i.e., −CO−NH−. The fact that the depletion of both −N═C═O and BZ bands was in contrast with the increment of −CO−NH− that could suggest the reaction between −N═C═O and −OH. The proposed reaction pathway is elaborated in Scheme 3. At the beginning of the curing process, the ring-opening reaction of some oxazine rings afforded the oligomer containing phenolic hydroxyl groups (i.e., −OH), and with the increase of the temperature, the reaction between −N═C═O and −OH and the cure of BZ occurred simultaneously and formed cross-linked polymer. Owing to such reaction, the adhesion between PBZ and MWNT could be improved.

The concentration effect of MWNT on the BZ curing temperature is summarized in Table 2. Increasing the MWNT concentration decreased the onset and the maximum curing temperature of BZ. This could attribute to the catalytic effect of MWNT surface −COOH groups on the BZ ring-opening reaction [69]. Increase of the concentration of modified-MWNT was equal to the introduction of high concentration of carboxyl group, which accelerated the BZ monomer curing occurred at the lower temperature.

Table 2
The effect of MWNT concentration on the BZ curing temperature

	MWNT	Exotherm		
	Content (wt%)	Onset (°C)	Maximum (°C)	Enthalpy (J/g)
BZ	−	252	258	309
BZ/MWNT	0.2	248	252	295
	0.5	245	250	293
	1	240	248	286
	1.5	238	247	298
	2	239	247	297

3.3. Dispersion of MWNT in PBZ matrix

The distribution of MWNT inside the PBZ matrix was examined by SEM and TEM. The SEM images of the fracture surface of nanocomposites are shown in Fig. 7. The uniform dispersion of MWNT (white dots as the black arrows indicated) inside the PBZ polymer matrix was observed regardless of the concentration of MWNT at 1 or 2 wt%. Some small areas of the extended white structures could be observed which were likely as the results of the amorphous carbon parts in the nanotube material, the impurities in the matrix or the fragments of the sample. The TEM images of the composites with various concentrations of MWNT are shown in Fig. 8. The homogenous dispersion of MWNT (black tubes) on the nano-scale level was noticed. The tubes were found as single ones and were less entangled than in the masterbatch, without any serious agglomeration or clusters. Moreover the random orientation of MWNT was observed inside the PBZ matrix. The slightly cloudy appearance could arise from small thickness differences within the thin sections. With the comparison of Fig. 8(a) and (b), it could be found that the distribution of MWNT was slightly more homogeneous in the nanocomposite with lower MWNT content. Increasing the concentration of MWNT to above 2 wt% could result in the aggregation of

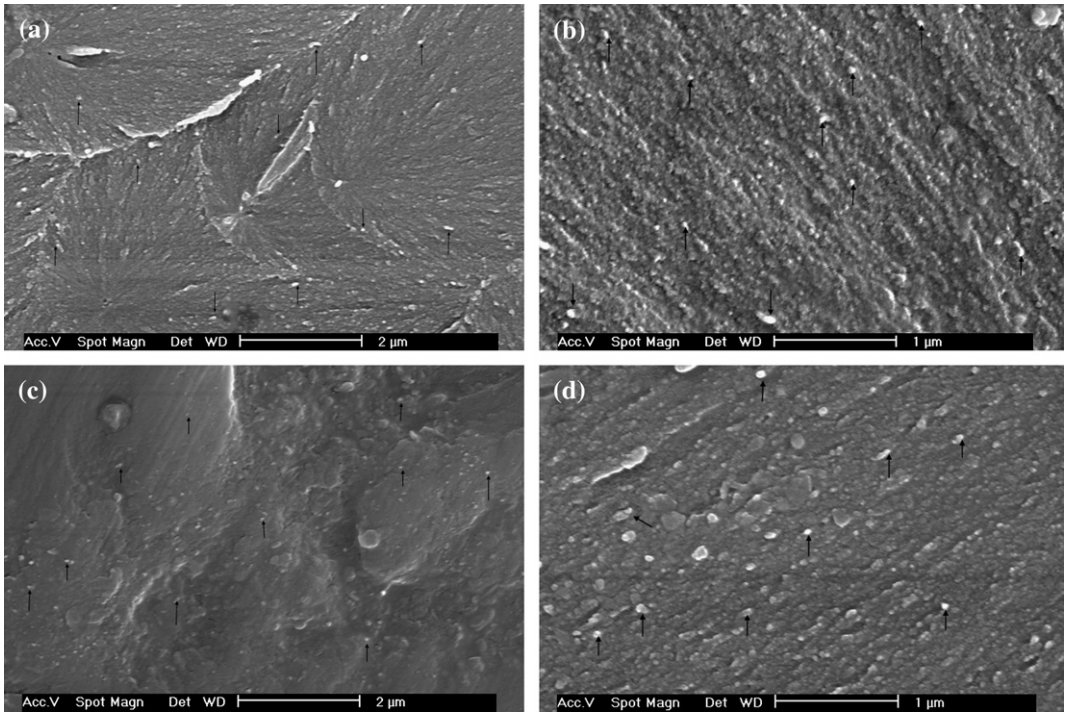

Fig. 7. SEM micrographs of the fracture surface of PBZ/MWNT nanocomposites: (a) and (b) 1 wt% MWNT; (c) and (d) 2 wt% MWNT.

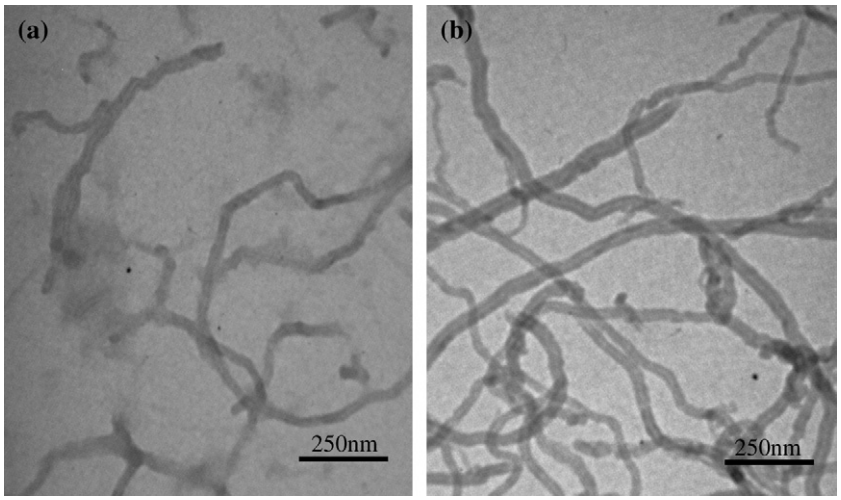

Fig. 8. TEM photos of PBZ/MWNT nanocomposites (a) 1 wt% MWNT and (b) 2 wt% MWNT.

it. This behavior should attribute to the high aspect ratio of the nanotube material and the hydrophilic groups (carboxyl groups) on MWNT surface, which were introduced during the process of the acid treatment.

3.4. Dynamic mechanical analysis of MWNT/PBZ nanocomposites

Fig. 9 shows the MWNT concentration effect on the storage modulus (E') of MWNT/PBZ nanocomposites obtained from dynamic mechanical analysis. Addition of MWNT into PBZ matrix caused the increase of E'. When the concentration of MWNT was 1 wt%, the E' of the nanocomposite at 50 °C reached 3.11 GPa, which was nearly three times higher than that of the pristine PBZ (1.09 GPa). It was generally accepted that the maximum adhesion effect between the polymer matrix and MWNT could occur due to the nanosize of CNTs. Thus, an immobilized PBZ layer could form around MWNT, which restricted the segmental motion of the polymer and resulted in the higher E'. The other reason for this result might be the augmentation of cross-link density compared with the matrix, which was caused by the reaction between the isocyanate groups on the MWNT surface and the phenolic hydroxyl groups generated by the ring opening of benzoxazine. In addition, the composites also exhibited significantly higher modulus above 200 °C, this behavior could attribute to the existence of stiff CNTs in PBZ resin and the chemical bonds between the MWNT and the PBZ matrix. With the increase of MWNT concentration, however, the aggregation of nanotubes took place and resulted in the decrease of E' at 50 °C for 2 wt% nanocomposite as compared with 1 wt% one.

The MWNT concentration effect on the glass transition temperature (T_g) of nanocomposites is shown in Fig. 10. The T_g was obtained from both the maximum of loss modulus (E'') and tan δ. Although tan δ calculation gave higher results than E'', the similar tendency of T_g was observed. When the MWNT concentration was less than 1.5 wt%, the glass transition of nanocomposite shifted towards higher temperature with

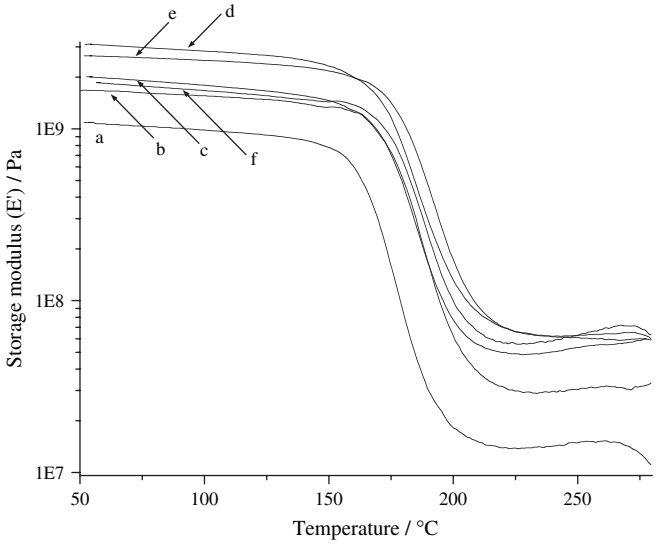

Fig. 9. MWNT concentration effect on the storage modulus (E') of nanocomposites: (a) 0, (b) 0.2 wt%, (c) 0.5 wt%, (d) 1 wt%, (e) 1.5 wt% and (f) 2 wt%.

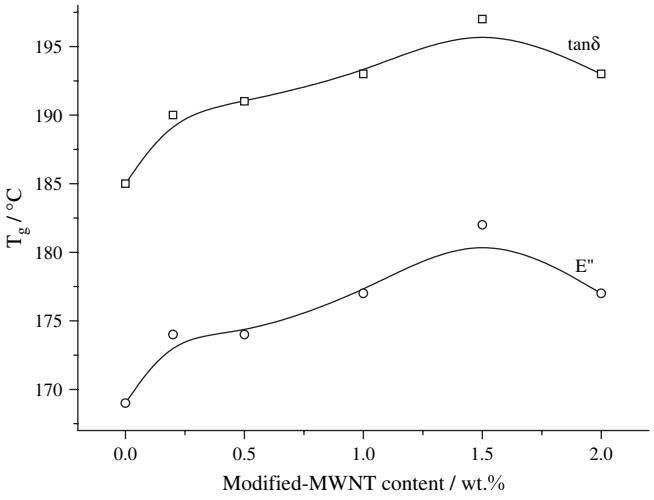

Fig. 10. MWNT concentration effect on the T_g of nanocomposites.

the increase of the MWNT concentration. However, further increasing the MWNT concentration to 2.0 wt% decreased the T_g of nanocomposite. The reasons for the increase of T_g should be, as mentioned above, significant nanoreinforcement effect of the MWNT and augmentation of cross-link density due to the reaction between isocyanate and phenolic hydroxyl groups, which could restrict the motion of the macromolecular chains and thus higher temperatures were required to provide the requisite thermal energy for the occurrence of a glass transition in nanocomposite [12,70]. The decrease of T_g was considered to be associated with the aggregation of the MWNT with higher concentration, which could weaken the stiffening effect of MWNT.

4. Conclusion

A novel nanocomposite consisted of uniformly dispersed MWNT in PBZ matrix was successfully prepared. The surface modification of MWNT, including nitric acid modification followed by toluene-2,4-diisocyanate (TDI) treatment, introduced hydroxyl, carboxyl, and isocyanate groups on the MWNT surface. Due to the catalytic effect of MWNT surface –COOH groups on the ring opening of benzoxazine, the curing temperature of BZ is lowered by the MWNT loading. The isocyanate groups reacted with the phenolic hydroxyl groups generated by the ring opening of benzoxazine, which resulted in the significant improvement of the adhesion between PBZ and MWNT. A well dispersed modified-MWNT on the nanoscale level inside PBZ matrix was observed by TEM and SEM. Dynamic mechanical analyses indicated the increase of storage modulus as well as T_g by the addition of MWNT into PBZ.

Acknowledgements

The authors gratefully acknowledge the support of this research by the Committee of the Natural Science Foundation of China (grant number 50473041).

References

[1] Iijima S. Nature 1991;354:56–8.
[2] Thostenson E, Ren Z, Chou TW. Compos Sci Technol 2001;61(13): 1899–912.
[3] Goze C, Bernier P, Henrard L, Vaccarini L, Hernandez E, Rubio A. Synth Met 1999;103(1–3):2500–1.
[4] Wong EW, Sheehan PE, Lieber CM. Science 1997;277:1971–5.
[5] Yao Z, Zhu CC, Cheng M, Liu J. Comput Mater Sci 2001;22:180–4.
[6] Yu MF, Files BS, Arepalli S, Ruoff RS. Phys Rev Lett 2000;84(24): 5552–5.
[7] Robertson DH, Brenner DW, Mintmire JW. Phys Rev B 1992;45:12592–5.
[8] Yakobson BI, Brabec CJ, Bernholc J. Phys Rev Lett 1996;76:2511–4.
[9] Lu JP. Phys Rev Lett 1997;79:1297–300.
[10] Cornwell CF, Wille LT. Solid State Commun 1997;101:555–8.
[11] Subramoney S. Adv Mater 1998;10(15):1157–71.
[12] Salvetat JP, Briggs GAD, Bonard JM, Bacsa RR, Kulik AJ, Stöckli T, et al. Phys Rev Lett 1999;82(5):944–7.
[13] Salvetat JP, Kulik AJ, Bonard JM, Briggs GAD, Stockli T, Metenier K, et al. Adv Mater 1999;11(2):161–5.
[14] Chapelle ML, Stephan C, Nguyen TP, Lefrant S, Journet C, Bernier P, et al. Synth Met 1999;103(1–3):2510–2.
[15] Chen J, Harmon MA, Hu H, Chen Y, Rao AM, Eklund PC, et al. Science 1998;282:95–8.
[16] Mickelson ET, Huffman CB, Finzler AG, Smalley RE, Hauge RH, Margrave JL. Chem Phys Lett 1998;296(1–2):188–94.
[17] Park C, Ounaies Z, Watson KA, Crooks RE, Smith J, Lowther SE, et al. Chem Phys Lett 2002;364(3–4):303–8.
[18] Huang S, Mau AWH, Turney TW, White PA, Dai L. J Phys Chem B 2000;104(10):2193–200.
[19] Jin ZX, Sun X, Xu GQ, Goh SH, Ji W. Chem Phys Lett 2000;318(6): 505–10.
[20] Fan JH, Wan MX, Zhu DB, Chang BH, Pan ZW, Xie SS. Synth Met 1999;102(1–3):1266–7.
[21] Fan JH, Wan MX, Zhu DB, Chang BH, Pan ZW, Xie SS. J Appl Polym Sci 1999;74(11):2605–10.
[22] Tang BZ, Xu HY. Macromolecules 1999;32(8):2569–76.
[23] Musa I, Baxendale M, Amaratunga GAJ, Eccleston W. Synth Met 1999; 102(1–3):1250.
[24] Pötschke P, Bhattacharyya AR, Janke A, Goering H. Compos Interfaces 2003;10(4–5):389–404.
[25] Pötschke P, Bhattacharyya AR, Janke A. Carbon 2004;42(5–6):965–9.
[26] Pötschke P, Dudkin SM, Alig I. Polymer 2003;44(17):5023–30.
[27] Pötschke P, Bhattacharyya AR, Janke A. Eur Polym J 2004;40(1): 137–48.
[28] Pötschke P, Fornes TD, Paul DR. Polymer 2002;43(11):3247–55.
[29] Pötschke P, Brünig H, Janke A, Fischer D, Jehnichen D. Polymer 2005; 46(23):10355–63.
[30] McNally T, Pötschke P, Halley P, Murphy M, Martin D, Bell SEJ, et al. Polymer 2005;46(19):8222–32.
[31] Kim GM, Michler GH, Pötschke P. Polymer 2005;46(18):7346–51.
[32] Pötschke P, Mahmoud A-G, Alig I, Dudkin S, Lellinger D. Polymer 2004;45(26):8863–70.
[33] Sandler J, Shaffer MSP, Prasse T, Bauhofer W, Schulte K, Windle AH. Polymer 1999;40(21):5967–71.
[34] Zeng H, Gao C, Wang Y, Watts PCP, Kong H, Cui X, et al. Polymer 2006;47(1):113–22.
[35] Kong H, Luo P, Gao C, Yan D. Polymer 2005;46(8):2472–85.
[36] Martin CA, Sandler JKW, Shaffer MSP, Schwarz MK, Bauhofer W, Schulte K, et al. Compos Sci Technol 2004;64(15):2309–16.
[37] Cai H, Yan FY, Xue QJ. Mater Sci Eng A 2004;364(1–2):94–100.
[38] Zhao LP, Gao L. Carbon 2004;42(2):423–60.
[39] Maser WK, Benito AM, Callejas MA, Seeger T, Martínez MT, Schreiber J, et al. Mater Sci Eng C 2003;23(1–2):87–91.
[40] Kashiwagi T, Grulke E, Hilding J, Groth K, Harris R, Butler K, et al. Polymer 2004;45(12):4227–39.
[41] Gong X, Liu J, Baskaran S, Voise RD, Young JS. Chem Mater 2000; 12(4):1049–52.
[42] Ferguson DW, Bryant EWS, Fowler HC. ESD thermoplastic product offers advantages for demanding electronic applications, ANTEC'98; 1998. p. 1219–22.
[43] Jin ZX, Pramoda KP, Xu GQ, Goh SH. Chem Phys Lett 2001;337(1–3): 43–7.
[44] Qian D, Dickey EC, Andrews R, Rantell T. Appl Phys Lett 2000;76(20): 2868–70.
[45] Schadler LS, Giannaris SC, Ajayan PM. Appl Phys Lett 1998;73(26): 3842–4.
[46] Biercuk MJ, Llaguno MC, Radosavljevic M, Hyun JK, Johnson AT, Fischer JE. Appl Phys Lett 2002;80(15):2767–9.
[47] Ishida H, Allen DJ. J Polym Sci Part B Polym Phys 1996;34(6):1019–30.
[48] Ishida H, Krus CM. Macromolecules 1998;31(8):2409–18.
[49] Wan XB, He JB, Xu N. Chem J Chinese Univ (Chinese) 2002;22(3):506–7.
[50] Ishida H, Sanders DP. Macromolecules 2000;33(22):8149–57.
[51] Agag T, Takeichi T. Macromolecules 2001;34(21):7257–63.
[52] Shen SB, Ishida H. J Polym Sci Part B Polym Phys 1999;37(23): 3257–68.
[53] Gu Y. Thermosetting Resin (Chinese) 2002;17(2):31–4.
[54] Agag T, Takeichi T. Macromolecules 2003;36(16):6010–7.

[55] Xin N, Ishida H. J Polym Sci Part B Polym Phys 1994;32(5):921–7.
[56] Ishida H, Low HY. J Appl Polym Sci 1998;69(13):2559–67.
[57] Jang J, Yang H. J Mater Sci 2000;35(9):2297–303.
[58] Jang J, Yang H. Compos Sci Technol 2000;60(3):457–63.
[59] Ishida H. Mater Res Innovations 2001;4(2–3):187–96.
[60] Yu DS, Shi ZX, Xu RW, Wang YZ. Chem J Chinese Univ (Chinese) 2002;23(11):2188–91.
[61] Shi ZX, Yu DS, Wang YZ, Xu RW. Eur Polym J 2002;38(4):727–33.
[62] Shi ZX, Yu DS, Wang YZ, Xu RW. J Appl Polym Sci 2003;88(1): 194–200.
[63] Agag T, Takeichi T. Polymer 2000;41(19):7083–90.
[64] Takeichi T, Zeidam R, Agag T. Polymer 2002;43(1):45–53.
[65] Lee YJ, Kuo SW, Su YC, Chen JK, Tu CW, Chang FC. Polymer 2004; 45(18):6321–31.
[66] Lee YJ, Huang JM, Kuo SW, Chen JK, Chang FC. Polymer 2005;46(7): 2320–30.
[67] Ning X, Ishida H. J Polym Sci Part A Polym Chem 1994;32(6):1121–9.
[68] Ishida H, Allen D. Polymer 1996;37(20):4487–95.
[69] Dunkers J, Ishida H. Polymerization of benzoxazine based phenolic resins with strong and weak carboxylic acids and phenols as catalysts. In: Fifty-fourth annual technical conference. Indianapolis, Indiana: SPE; 1996.
[70] Bansal A, Yang H, Li C, Cho K, Benicewicz BC, Kumar SK, et al. Nature Mater 2005;4(9):693–8.